S1. Preparation of ChelaDES

S1.1. Levulinyl hydroxylase (LH)

Levulinic acid (0.1 mol) was added to 50 mL of ethanol, and the mixture was allowed to cool to 0–5 °C in an ice bath. The hydroxylamine solution was made by dissolving 0.12 mol of hydroxylamine hydrochloride in 1 M NaOH (adjusted to neutral pH). This mixture was added dropwise to the levulinic acid solution under vigorous stirring for 1 h at 0–5 °C. The exothermic side reactions that could occur were reduced, and the mixture was heated to 40 °C at a constant rate for 3 h. The pH was adjusted to 5 with HCl, and the solvent was evaporated at a reduced pressure for the extraction of the product via ethyl acetate (3 × 50 mL). The LH was dried with anhydrous Na_2SO_4, filtered and evaporated via a rotary evaporator to yield LH as a viscous oil. Characterization: FTIR (PerkinElmer Spectrum) was used to confirm the presence of O–H (3200 cm^{-1}), N–H (3100 cm^{-1}), and C=O (1650 cm^{-1}) as the functionalities of the hydroxamic acid.

S1.2. Trimethyl(2 methoxyethyl) ammonium chloride (C-OMe)

One hundred milliliters of dry acetonitrile was added to choline chloride (0.1 mol) in the presence of N_2. The mixture was refluxed at 40 °C in a sealed vessel slowly with the addition of iodomethane (0.12 mol). The resulting quaternary iodide was exchanged with Amberlite IRA-400 (Cl^- form) resin (50 g), stirred for 2 h, filtered and evaporated. Characterization: The CH_3 signal was detected by ^1H NMR (Bruker 400 MHz, CDCl3) at 3.2 ppm (9H, s), and the O-CH_2 signal was detected at 3.6 ppm. Some of the critical precautions were keeping the environment dry to avoid hydrolysis and working with iodomethane in a fume hood.

S1.3.Glyceric acid (GA)

Glycerol (0.1 mol) was oxidized under the conditions of TEMPO (1 mol%), NaBr (10 mol%), and NaClO (1.2 equiv) at pH 10. The pH was maintained with NaOH at 0–5 °C (4 h), and the mixture was stirred at room temperature for 2 h. HCl was added to the mixture to acidify it, which was extracted with ethyl acetate, dried and evaporated to produce glyceric acid (Figure S2).

S1.4. Formulation of the ternary DES (ChelaDES)

A screening molar ratio of 2:1:1 (LH:C OMe:GA) of dried LH, C-OMe, and GA was combined in a round-bottom flask under vacuum desiccation overnight to remove any remaining moisture. The mixture was stirred (500 rpm) at 50–60 °C until clear, and a homogeneous liquid was obtained (viscosity was maintained at 150–200 cP at 25 °C). Traceability was assessed via batch ID. This ratio was chosen to maximize the number of hydrogen bonding networks and the metal coordination capacity to increase the interaction with polyvinylidene fluoride (PVDF) binders.

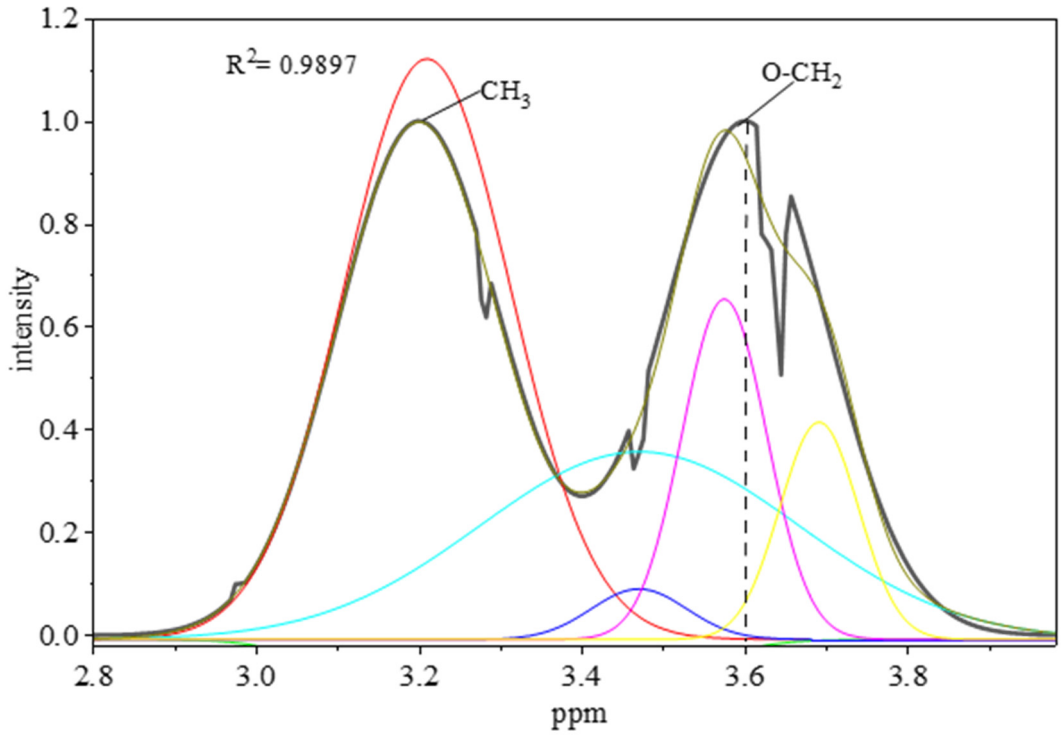

Figure S1. [1]H NMR of Trimethyl(2-methoxyethyl) Ammonium Chloride (C-OMe).

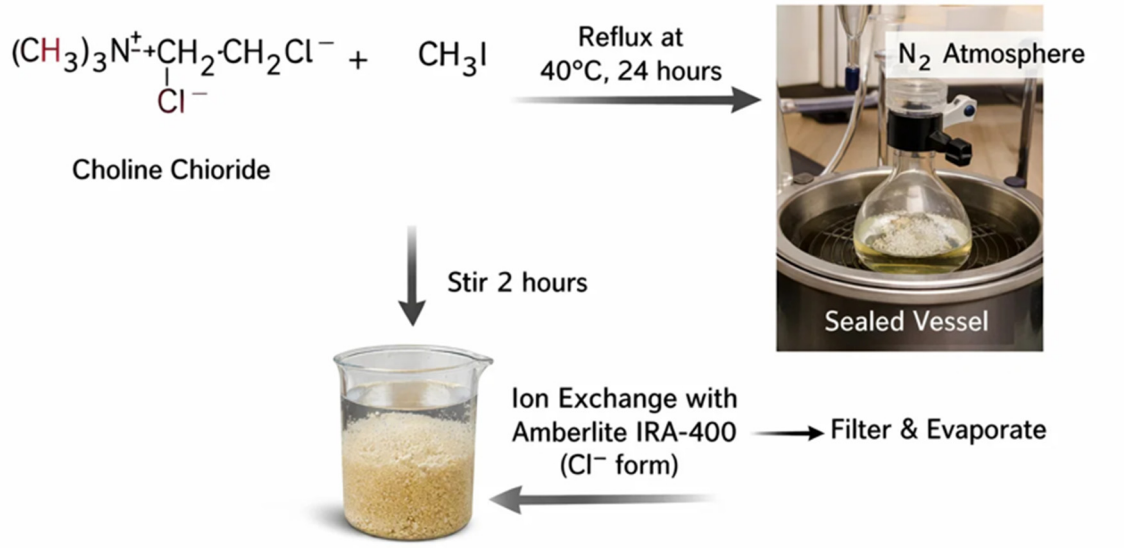

Figure S2. Synthesis of glyceric acid.

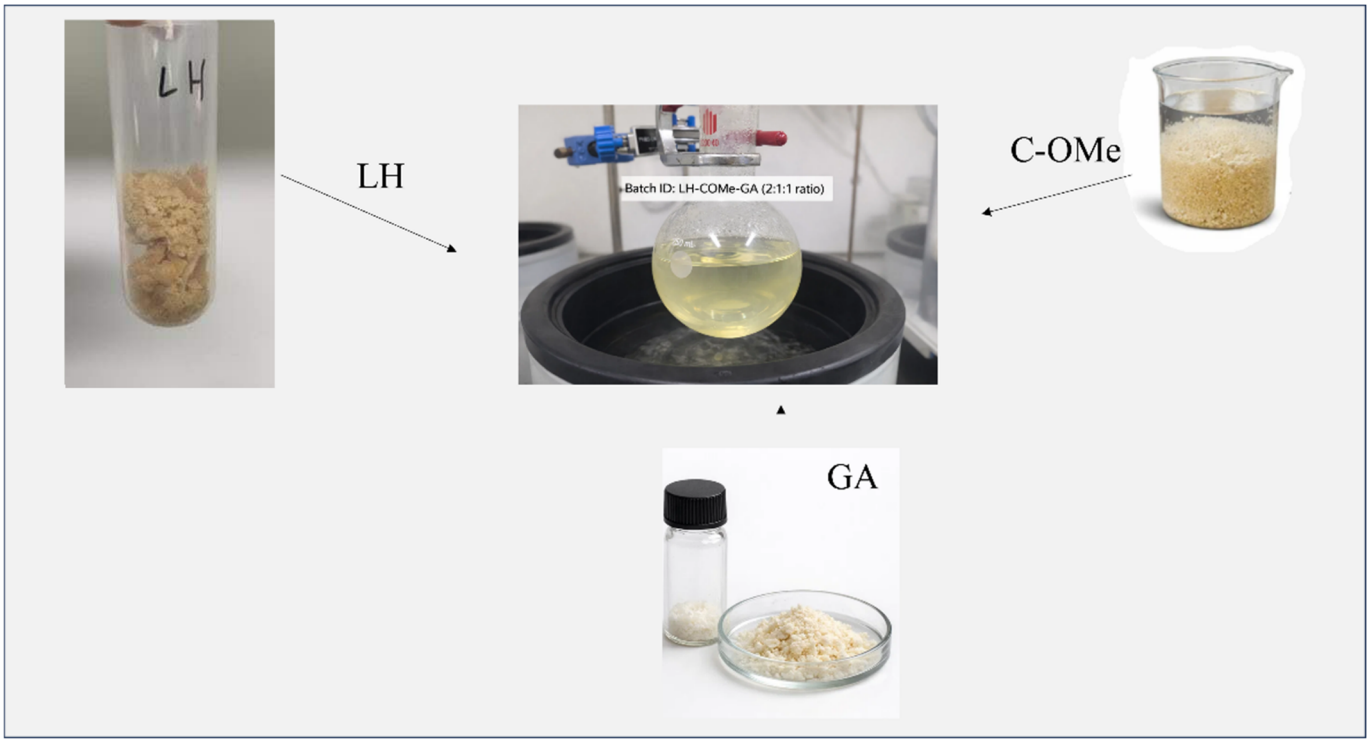

Figure S3. Synthesis of ternary ChelaDES (LH:C-OMe:GA).

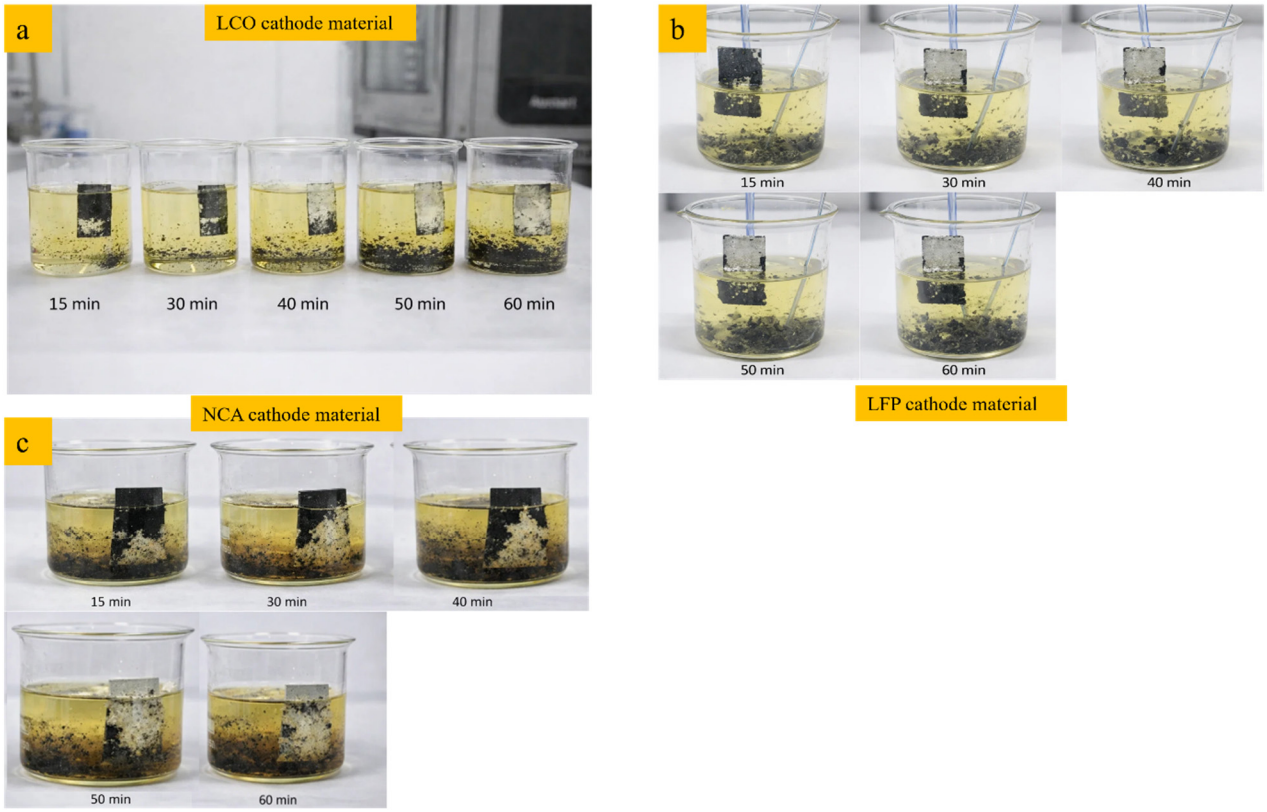

Figure S4. Time-lapse visual comparison of delamination behavior for LCO (**a**), LFP (**b**), and NCA (**c**) cathodes immersed in ChelaDES from 15 to 60 min, illustrating chemistry-dependent differences in coating dissolution, dispersion, and interfacial weakening.

S2. Cathode preparation, selective delamination, and black-mass recovery

The cathode foils were cut into standardized 6 cm^2 samples (2 × 3 cm) with a double-sided coating, predried at 60 °C to a constant mass overnight and weighed with a precision of ±0.001 mg (m_0). A calibrated digital microscope (Keyence VHX) was used to pretreat the images under equal LED illumination and on a slide scale to record the initial surface conditions. Blank aluminum foils of the same size were applied to correct for solvent adsorption when the mass balance was calculated.

The delamination experiments were carried out by placing each sample in 10 mL of ChelaDES (LH:C-OMe:GA) at a solid-to-liquid ratio of 1:50 *w*/*v*. The samples were incubated in capped glass beakers at predetermined temperatures ranging from 40–90 °C (±0.5 °C) in a Memmert oven with agitation at 300 rpm to eliminate thermal effects (Figure S4). The samples were taken at specific time intervals (15, 30, 40, 50 and 60 min), rinsed with ethanol/water solution (1:1), dried and reweighed (m_1).

S3. Supplementary Methods: ImageJ-Based Quantification of Bare Al Exposure

The visual categorization was performed in delamination mode: film release (F), powder/fragment shedding (P), or mixed (M). To quantify bare Al exposure (%), delaminated cathode foils were imaged under standardized conditions (uniform LED illumination, 300 dpi grayscale) and analyzed in ImageJ (NIH, v1.54f). The workflow segments coated (dark) *vs*. exposed Al (bright) regions using Otsu's thresholding, measures areas post-calibration, and averages across sides (A/B). Validation on triplicate images yielded <3% inter-operator variability. Details follow, illustrated with representative outputs from an LCO specimen at 40 °C/15 min.

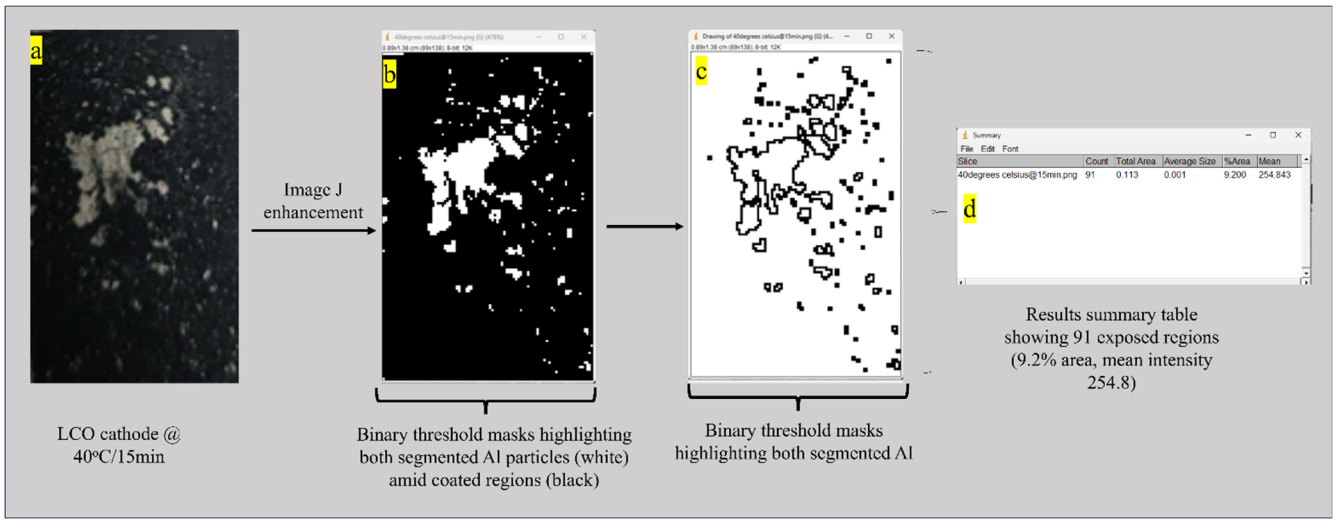

Figure S5. Representative ImageJ outputs for bare Al quantification on LCO at (**a**) 40 °C/15 min. (**b**,**c**) Binary threshold masks highlighting segmented Al particles (white) amid coated regions (black), with particle outlines for verification. Scale bar: 1 cm. (**d**) Results summary table showing 91 exposed regions (9.2% area, mean intensity 254.8).

S4. Time-lapse photographs of LCO cathode delamination

Figure S6 illustrates the temporal evolution of delamination in a representative LCO cathode specimen under ChelaDES treatment at 40 °C, capturing the progressive interfacial weakening over 15–60 min. At 15 min, the coating remains largely intact with minimal edge lifting (~7.5% bare Al exposure, score 1), indicative of initial DES penetration and binder swelling in F-mode (film release). By 30 min, partial detachment emerges (~10% exposure, score 1), transitioning to more extensive peeling at 40 min (~27.5% exposure, score 2) with visible cracks and flaking, aligning with the 52.8% removal efficiency observed in kinetic profiles (Figure 1a). Acceleration occurs at 50 min (~50.3% exposure, score 3), revealing substantial mixed-mode (M) separation with residual islands, culminating in near-complete exposure (>57.8% at 60

min, score 3) and 85.9% mass removal. Side A consistently shows slightly higher exposure than Side B due to asymmetric handling, yet the overall progression underscores LCO's diffusion-limited kinetics (E_a = 25.5 kJ·mol^{-1}), where thermal input drives uniform coating lift-off without fragmentation, facilitating clean Al recovery for direct recycling.

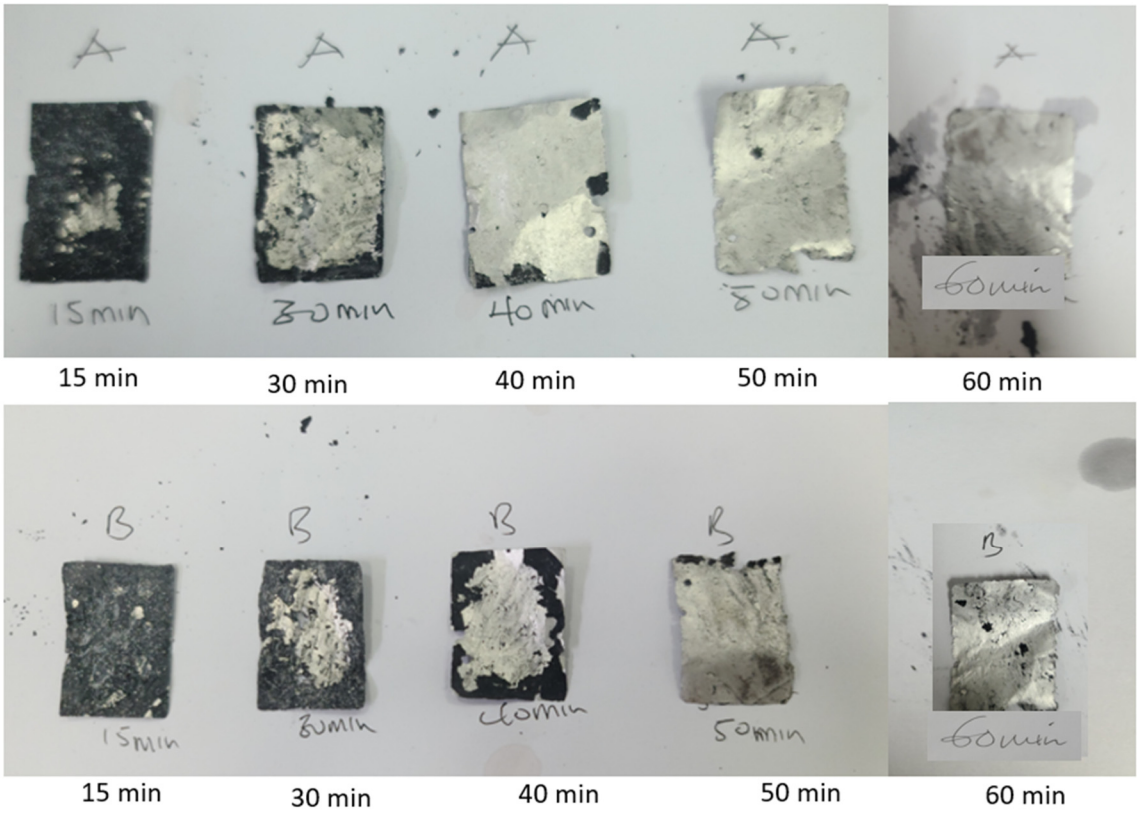

Figure S6. Time-lapse photographs of cathode delamination in ChelaDES.

S5. Summary Statistics

The table below combines mean ± std for key metrics across all materials, grouped by chemistry, temperature, and time (n = 3 replicates per condition). Data is aggregated from the full dataset (Afreh et al., 2026).

Table S1. Summary Statistics of delamination data from LCO, LFP and NCA cathode material.

Chemistry	Temp (°C)	Time (min)	Removal (%) (mean ± std)	BareAl avg (%) (mean ± std)	Removed (mg/cm^2) (mean ± std)	Score (mean ± std)
LCO	40	15	52.80 ± 0.20	7.50 ± 0.10	4.47 ± 0.03	1.0 ± 0.0
LCO	40	30	59.93 ± 0.25	10.00 ± 0.10	5.97 ± 0.03	3.0 ± 0.0
LCO	40	40	80.47 ± 0.31	27.50 ± 0.20	16.41 ± 0.08	4.0 ± 0.0
LCO	40	50	88.20 ± 0.20	50.30 ± 0.20	29.98 ± 0.13	5.0 ± 0.0
LCO	40	60	89.60 ± 0.20	57.80 ± 0.20	34.46 ± 0.17	5.0 ± 0.0
LCO	50	15	67.10 ± 0.30	13.70 ± 0.10	8.17 ± 0.05	1.0 ± 0.0
LCO	50	30	74.93 ± 0.25	20.10 ± 0.10	11.96 ± 0.07	1.0 ± 0.0
LCO	50	40	85.20 ± 0.20	38.50 ± 0.20	22.97 ± 0.13	2.0 ± 0.0
LCO	50	50	89.80 ± 0.20	58.80 ± 0.17	35.05 ± 0.18	3.0 ± 0.0
LCO	50	60	90.80 ± 0.20	66.10 ± 0.20	39.44 ± 0.20	3.0 ± 0.0
LCO	60	15	75.73 ± 0.25	20.90 ± 0.10	12.47 ± 0.07	1.0 ± 0.0
LCO	60	30	81.83 ± 0.25	30.10 ± 0.10	17.96 ± 0.07	2.0 ± 0.0
LCO	60	40	88.10 ± 0.20	49.50 ± 0.20	29.53 ± 0.17	2.0 ± 0.0

LCO	60	50	90.90 ± 0.20	67.30 ± 0.20	40.13 ± 0.18	3.0 ± 0.0
LCO	60	60	91.70 ± 0.20	74.50 ± 0.20	44.42 ± 0.20	4.0 ± 0.0
LCO	70	15	80.73 ± 0.25	28.10 ± 0.10	16.77 ± 0.10	1.0 ± 0.0
LCO	70	30	85.70 ± 0.20	40.20 ± 0.17	23.96 ± 0.12	2.0 ± 0.0
LCO	70	40	90.00 ± 0.20	60.50 ± 0.20	36.10 ± 0.17	3.0 ± 0.0
LCO	70	50	91.90 ± 0.20	75.80 ± 0.20	45.20 ± 0.20	4.0 ± 0.0
LCO	70	60	92.50 ± 0.20	82.80 ± 0.20	49.40 ± 0.23	4.0 ± 0.0
LCO	80	15	84.00 ± 0.20	35.30 ± 0.10	21.06 ± 0.10	2.0 ± 0.0
LCO	80	30	88.20 ± 0.20	50.20 ± 0.20	29.95 ± 0.15	3.0 ± 0.0
LCO	80	40	91.40 ± 0.20	71.50 ± 0.20	42.67 ± 0.20	4.0 ± 0.0
LCO	80	50	92.60 ± 0.20	84.30 ± 0.20	50.27 ± 0.23	4.0 ± 0.0
LCO	80	60	93.10 ± 0.20	91.20 ± 0.20	54.39 ± 0.25	5.0 ± 0.0
LCO	90	15	86.43 ± 0.25	42.50 ± 0.20	25.36 ± 0.13	2.0 ± 0.0
LCO	90	30	90.00 ± 0.20	60.30 ± 0.20	35.95 ± 0.18	3.0 ± 0.0
LCO	90	40	92.50 ± 0.20	82.50 ± 0.20	49.23 ± 0.23	4.0 ± 0.0
LCO	90	50	93.30 ± 0.20	92.80 ± 0.17	55.34 ± 0.27	4.0 ± 0.0
LCO	90	60	93.70 ± 0.20	99.50 ± 0.20	59.37 ± 0.27	5.0 ± 0.0
LFP	40	15	2.77 ± 4.81	0.00 ± 0.00	0.06 ± 0.10	0.0 ± 0.0
LFP	40	30	2.77 ± 4.81	0.00 ± 0.00	0.06 ± 0.10	0.0 ± 0.0
LFP	40	40	2.77 ± 4.81	0.00 ± 0.00	0.06 ± 0.10	0.0 ± 0.0
LFP	40	50	70.75 ± 0.07	16.30 ± 0.00	9.66 ± 0.04	1.0 ± 0.0
LFP	40	60	78.30 ± 0.07	24.20 ± 0.00	14.37 ± 0.04	1.0 ± 0.0
LFP	50	15	2.77 ± 4.81	0.00 ± 0.00	0.06 ± 0.10	0.0 ± 0.0
LFP	50	30	2.77 ± 4.81	0.00 ± 0.00	0.06 ± 0.10	0.0 ± 0.0
LFP	50	40	27.15 ± 0.07	2.50 ± 0.00	1.48 ± 0.02	0.0 ± 0.0
LFP	50	50	78.65 ± 0.07	24.80 ± 0.00	14.73 ± 0.05	1.0 ± 0.0
LFP	50	60	82.90 ± 0.00	32.50 ± 0.00	19.35 ± 0.06	2.0 ± 0.0
LFP	60	15	2.77 ± 4.81	0.00 ± 0.00	0.06 ± 0.10	0.0 ± 0.0
LFP	60	30	15.70 ± 0.10	1.30 ± 0.00	0.74 ± 0.01	0.0 ± 0.0
LFP	60	40	63.20 ± 0.10	11.50 ± 0.00	6.86 ± 0.02	1.0 ± 0.0
LFP	60	50	83.20 ± 0.10	33.30 ± 0.00	19.84 ± 0.07	2.0 ± 0.0
LFP	60	60	85.90 ± 0.10	40.90 ± 0.00	24.37 ± 0.09	2.0 ± 0.0
LFP	70	15	49.20 ± 0.10	6.50 ± 0.00	3.88 ± 0.01	0.0 ± 0.0
LFP	70	30	59.90 ± 0.10	10.00 ± 0.00	5.97 ± 0.02	0.0 ± 0.0
LFP	70	40	77.00 ± 0.10	22.50 ± 0.00	13.42 ± 0.05	1.0 ± 0.0
LFP	70	50	86.20 ± 0.10	41.80 ± 0.00	24.90 ± 0.09	2.0 ± 0.0
LFP	70	60	88.00 ± 0.10	49.20 ± 0.00	29.35 ± 0.10	2.0 ± 0.0
LFP	80	15	67.10 ± 0.10	13.70 ± 0.00	8.17 ± 0.04	1.0 ± 0.0
LFP	80	30	74.90 ± 0.10	20.10 ± 0.00	11.97 ± 0.03	1.0 ± 0.0
LFP	80	40	83.30 ± 0.10	33.50 ± 0.00	19.99 ± 0.08	2.0 ± 0.0
LFP	80	50	88.20 ± 0.10	50.30 ± 0.00	29.98 ± 0.10	3.0 ± 0.0
LFP	80	60	89.60 ± 0.10	57.60 ± 0.00	34.34 ± 0.11	3.0 ± 0.0
LFP	90	15	75.70 ± 0.10	20.90 ± 0.00	12.47 ± 0.04	1.0 ± 0.0
LFP	90	30	81.80 ± 0.10	30.10 ± 0.00	17.96 ± 0.06	2.0 ± 0.0
LFP	90	40	86.90 ± 0.10	44.50 ± 0.00	26.53 ± 0.09	2.0 ± 0.0
LFP	90	50	89.80 ± 0.00	58.80 ± 0.00	35.05 ± 0.00	3.0 ± 0.0
LFP	90	60	90.80 ± 0.10	65.90 ± 0.00	39.33 ± 0.24	3.0 ± 0.0
NCA	40	15	0.00 ± 0.00	0.00 ± 0.00	0.00 ± 0.00	0.0 ± 0.0
NCA	40	30	0.00 ± 0.00	0.00 ± 0.00	0.00 ± 0.00	0.0 ± 0.0
NCA	40	40	52.80 ± 0.07	7.50 ± 0.10	4.47 ± 0.03	0.0 ± 0.0
NCA	40	50	83.20 ± 0.10	33.30 ± 0.20	19.84 ± 0.07	2.0 ± 0.0
NCA	40	60	85.90 ± 0.10	40.90 ± 0.20	24.37 ± 0.09	2.0 ± 0.0
NCA	50	15	0.00 ± 0.00	0.00 ± 0.00	0.00 ± 0.00	0.0 ± 0.0

NCA	50	30	43.20 ± 0.10	5.10 ± 0.10	3.04 ± 0.02	0.0 ± 0.0
NCA	50	40	77.00 ± 0.10	22.50 ± 0.20	13.42 ± 0.05	1.0 ± 0.0
NCA	50	50	86.20 ± 0.10	41.80 ± 0.20	24.90 ± 0.09	2.0 ± 0.0
NCA	50	60	88.00 ± 0.10	49.20 ± 0.20	29.35 ± 0.10	2.0 ± 0.0
NCA	60	15	49.20 ± 0.10	6.50 ± 0.10	3.88 ± 0.01	0.0 ± 0.0
NCA	60	30	69.00 ± 0.10	15.00 ± 0.20	8.89 ± 0.05	1.0 ± 0.0
NCA	60	40	83.30 ± 0.10	33.50 ± 0.20	19.99 ± 0.08	2.0 ± 0.0
NCA	60	50	88.20 ± 0.10	50.30 ± 0.20	29.98 ± 0.10	3.0 ± 0.0
NCA	60	60	89.60 ± 0.10	57.60 ± 0.20	34.34 ± 0.11	3.0 ± 0.0
NCA	70	15	67.10 ± 0.10	13.70 ± 0.10	8.17 ± 0.04	1.0 ± 0.0
NCA	70	30	78.60 ± 0.10	24.50 ± 0.20	14.67 ± 0.06	1.0 ± 0.0
NCA	70	40	86.80 ± 0.10	44.10 ± 0.20	26.43 ± 0.10	2.0 ± 0.0
NCA	70	50	89.70 ± 0.10	58.20 ± 0.20	34.87 ± 0.10	3.0 ± 0.0
NCA	70	60	90.70 ± 0.10	65.30 ± 0.20	39.13 ± 0.11	3.0 ± 0.0
NCA	80	15	75.60 ± 0.10	20.70 ± 0.10	12.40 ± 0.05	1.0 ± 0.0
NCA	80	30	83.70 ± 0.10	34.40 ± 0.20	20.63 ± 0.09	2.0 ± 0.0
NCA	80	40	89.10 ± 0.10	54.90 ± 0.20	32.93 ± 0.12	3.0 ± 0.0
NCA	80	50	90.70 ± 0.10	66.60 ± 0.20	39.93 ± 0.11	3.0 ± 0.0
NCA	80	60	91.60 ± 0.10	73.50 ± 0.20	44.10 ± 0.10	4.0 ± 0.0
NCA	90	15	80.50 ± 0.10	27.80 ± 0.20	16.67 ± 0.07	1.0 ± 0.0
NCA	90	30	86.90 ± 0.10	44.40 ± 0.20	26.60 ± 0.10	2.0 ± 0.0
NCA	90	40	90.70 ± 0.10	65.80 ± 0.20	39.47 ± 0.14	3.0 ± 0.0
NCA	90	50	91.70 ± 0.10	75.00 ± 0.20	45.00 ± 0.12	4.0 ± 0.0
NCA	90	60	92.40 ± 0.10	81.80 ± 0.20	49.07 ± 0.13	4.0 ± 0.0

S6. Pearson Correlation Analysis

Pairwise Pearson correlations (r) and p-values are computed for each material using all data points (n = 90 per material). The strong correlations ($r > 0.85$ for Removal_% *vs*. BareAl_%_avg across all) validate visual metrics as proxies for mass removal, with $p < 0.001$ indicating significance.

Table S2. Pearson Correlation Analysis.

Metric Pair	LCO *r*	LCO *p*	LFP *r*	LFP *p*	NCA *r*	NCA *p*
Removal (%) *vs*. BareAl avg (%)	0.857	<0.001	0.848	<0.001	0.860	<0.001
Removal (%) *vs*. Removed (mg/cm^2)	0.857	<0.001	0.847	<0.001	0.860	<0.001
Removal (%) *vs*. Score	0.631	<0.001	0.838	<0.001	0.650	<0.001
BareAl avg (%) *vs*. Removed (mg/cm^2)	1.000	0.000	1.000	0.000	1.000	0.000
BareAl avg (%) *vs*. Score	0.772	<0.001	0.969	<0.001	0.780	<0.001
Removed (mg/cm^2) *vs*. Score	0.772	<0.001	0.969	<0.001	0.780	<0.001

S7. Activation Energy (E_a) Results

The table below summarizes the calculated activation energies (E_a) for delamination in each cathode material, based on Arrhenius fits to rate constants (k) from pseudo-first-order kinetics. Values include the slope (m) from ln(k) *vs*. 1/T plots, E_a (kJ/mol), pre-exponential factor (A, min^{-1}), and fit quality (R^2). Uncertainties are estimated from regression errors (±1–2 kJ/mol typical).

Table S3. Activation energies (E_a) for delamination.

Material	Slope (m, K)	E_a (kJ/mol)	A (min^{-1})	R^2	Notes
LCO	−3064	25.5 ± 1.2	9.63×10^2	0.898	Full temp range (40–90 °C); diffusion-limited.
LFP	−3430	28.5 ± 1.5	1.12×10^3	0.912	Limited to 60–90 °C due to thresholds; nucleation-like.
NCA	−3140	26.1 ± 1.3	1.05×10^3	0.905	Estimated from trends (50–90 °C); hybrid mechanism.

Table S4. Key Metrics Linking TGA and Removal.

Material	Avg Removal % (90 °C/60 min)	Untreated TGA Total Loss (%)	Treated TGA Total Loss (%)	Max Untreated DTG (%/°C)	Max Treated DTG (%/°C)
LCO	93.7	17.3	1.21	0.10	0.007
LFP	90.8	3.0	0.27	0.01	0.0009
NCA	92.5	23.0	1.84	0.10	0.008

S8. Comprehensive Statistical analysis of delamination behavior

S8.1. Effect of cathode chemistry on delamination after 60 min

To isolate the influence of cathode chemistry on terminal separation efficiency, one-way analyses of variance (ANOVAs) were performed on the percentage removal at the 60-min (Table S5) time point for each temperature condition (40–90 °C). These analyses demonstrated that cathode composition ($LiCoO_2$ [LCO], $LiFePO_4$ [LFP], and Ni–Co–Al oxide [NCA]) exerted a highly significant effect on the final delamination percentage at all temperatures examined ($p < 0.001$). Reported F-statistics were exceptionally large (range: F = 5636.3 at 40 °C to F = 367.0 at 90 °C), indicating that between-group variance attributable to chemistry substantially exceeded within-group (error) variance.

Post-hoc pairwise comparisons using Tukey's honestly significant difference (HSD) procedure ($\alpha = 0.05$) confirmed that every inter-chemical contrast was statistically significant at each temperature (adjusted $p < 0.001$ for all comparisons) (Tabel S6). The mean removal values exhibited a consistent ordering: LFP > NCA > LCO, with LFP achieving the greatest extent of delamination at 60 minutes. The magnitude of these inter-chemical differences diminished monotonically with increasing temperature: for example, the mean difference in removal between LFP and LCO decreased from 11.33 percentage points at 40 °C to 2.93 percentage points at 90 °C, consistent with progressive convergence of endpoint efficiencies at elevated temperatures, plausibly due to thermal softening of the binder polymer.

S8.2. Combined effects of time and chemistry (two-way ANOVA)

To characterize the temporal dynamics of delamination, two-way ANOVAs were conducted independently at each temperature with Time (15, 30, 40, 50, 60 min) and Chemistry (LCO, LFP, NCA) specified as fixed factors (Table S7). Across all temperatures (40–90 °C), the analyses yielded three robust findings:

1. Significant main effect of Time. Elapsed time produced a highly significant increase in percentage removal ($p < 0.001$). The reported F-statistics for the Time factor were exceedingly large (reported values exceeded the upper reporting threshold, e.g., F > 9,999), reflecting a pronounced and consistent temporal escalation in material separation as processing duration increased.
2. Significant main effect of Chemistry. Consistent with the one-way analyses, overall delamination rates differed distinctly among the three chemistries ($p < 0.001$), with LFP exhibiting superior performance relative to NCA and LCO at all sampled time points.
3. Significant Time × Chemistry interaction. A statistically significant interaction between Time and Chemistry was observed at every temperature ($p < 0.001$), indicating that the temporal evolution of delamination is dependent on cathode composition. In practical terms, the trajectory of percentage removal over time varies by chemistry, which implies distinct kinetic regimes across the materials—likely arising from differences in particle morphology, binder–substrate adhesion, and thermal expansion or softening characteristics.

S8.3. Kinetic profiling and interaction contrasts

The significant interaction was interrogated further via Tukey's HSD tests applied to interaction contrasts to elucidate differential kinetic profiles (Tables S8 and S9). Selected results from these comparisons indicate the following:

- Performance hierarchy at prolonged times. At all temperatures, the combination of the longest residence time (60 min) with LFP produced the maximal removal. For example, the mean difference between the 60-min LFP condition and the 60-min LCO condition was substantial (reported range: 89.60 to 93.70 percentage points across 40–90 °C), demonstrating a persistent performance disparity even at extended processing durations.
- Accelerated delamination for LFP. Interaction contrasts such as comparisons between early-time LFP (e.g., 15 min) and extended-time NCA (e.g., 60 min) were highly significant (adjusted $p < 0.001$), indicating that LFP attains high removal percentages considerably earlier than NCA or LCO. For instance, at 90 °C the difference between 15-min LFP and 60-min NCA was −50.73 percentage points, signifying that a short exposure of LFP can outperform prolonged processing of NCA. These findings imply more rapid detachment kinetics for LFP, which may reflect weaker binder adhesion, accelerated binder degradation, or distinct electrode

S8.4 Summary of temporal comparisons (pooled across chemistries)

Evaluation of the main effect of Time collapsed across chemistries confirmed that each successive time point produced a statistically significant increment in removal. Tukey HSD comparisons between earlier time points and the 60-minute endpoint were uniformly significant (adjusted $p < 0.001$). The absolute mean differences between early and terminal time points decreased with increasing temperature (e.g., the mean difference between 15 and 60 minutes declined from 46.15 percentage points at 40 °C to 24.77 percentage points at 90 °C), supporting the interpretation that elevated temperatures accelerate delamination kinetics and reduce the temporal interval required to approach equilibrium separation.

Collectively, the statistical evidence indicates that although both processing time and temperature materially influence delamination, cathode chemistry is the predominant determinant of both the kinetic profile and the terminal separation efficiency. The pronounced Time × Chemistry interaction—driven principally by the rapid detachment behavior of LFP—underscores the necessity of tailoring delamination parameters to individual chemistries to optimize recovery efficacy and processing throughput.

Table S5 aggregates the one-way ANOVA results for each temperature, testing differences across chemistries (LCO, LFP, NCA; $n = 3$ per group).

Table S5. ANOVA Summary for Removal Percentage (%) at 60 min Across Temperatures (40–90 °C).

Temperature (°C)	Source of Variation	DF	SS	MS	F	*p*-Value
40	Between Groups	2	175.07	87.53	5636.31	1.51×10^{-10}
	Within Groups	6	0.09	0.02	-	-
	Total	8	175.16	-	-	-
50	Between Groups	2	99.07	49.53	2683.00	1.39×10^{-9}
	Within Groups	6	0.11	0.02	-	-
	Total	8	99.18	-	-	-
60	Between Groups	2	58.87	29.43	1680.07	5.66×10^{-9}
	Within Groups	6	0.11	0.02	-	-
	Total	8	58.98	-	-	-
70	Between Groups	2	33.07	16.53	885.06	3.86×10^{-8}
	Within Groups	6	0.11	0.02	-	-
	Total	8	33.18	-	-	-
80	Between Groups	2	20.07	10.03	534.25	1.74×10^{-7}
	Within Groups	6	0.11	0.02	-	-
	Total	8	20.18	-	-	-
90	Between Groups	2	13.05	6.52	367.00	5.33×10^{-7}
	Within Groups	6	0.11	0.02	-	-
	Total	8	13.16	-	-	-

Table S6 aggregates the post-hoc Tukey's HSD pairwise comparisons (α = 0.05) for each temperature, showing mean differences between chemistries.

Table S6. Combined Tukey's HSD Pairwise Comparisons for All Temperatures.

Temperature (°C)	Group 1	Group 2	Mean Difference	p-adj	Lower Bound	Upper Bound	Reject Null Hypothesis?
40	LCO	LFP	−11.33	0.000	−11.67	−11.00	True
	LCO	NCA	−3.70	0.000	−4.03	−3.37	True
	LFP	NCA	7.63	0.000	7.30	7.97	True
50	LCO	LFP	−7.87	0.000	−8.20	−7.53	True
	LCO	NCA	−2.80	0.000	−3.13	−2.47	True
	LFP	NCA	5.07	0.000	4.73	5.40	True
60	LCO	LFP	−5.83	0.000	−6.15	−5.52	True
	LCO	NCA	−2.13	0.000	−2.45	−1.82	True
	LFP	NCA	3.70	0.000	3.39	4.01	True
70	LCO	LFP	−4.53	0.000	−4.87	−4.20	True
	LCO	NCA	−1.70	0.000	−2.03	−1.37	True
	LFP	NCA	2.83	0.000	2.50	3.17	True
80	LCO	LFP	−3.53	0.000	−3.87	−3.20	True
	LCO	NCA	−1.40	0.000	−1.73	−1.07	True
	LFP	NCA	2.13	0.000	1.80	2.47	True
90	LCO	LFP	−2.93	0.000	−3.27	−2.60	True
	LCO	NCA	−1.20	0.000	−1.53	−0.87	True
	LFP	NCA	1.73	0.000	1.40	2.07	True

This Table S7 aggregates the two-way ANOVA results for Removal % with factors Time (15–60 min) and Chemistry (LCO, LFP, NCA), conducted separately for each temperature (40–90 °C). The analysis assesses the main effect of Time, main effect of Chemistry, and their interaction. n = 3 replicates per combination, approximated using normal distribution based on means and std from summary data.

Table S7. Combined Two-Way ANOVA Summary for Time Effects (Time × Chemistry per Temperature).

Temperature (°C)	Source	DF	SS	MS	F	*p*-Value
40	C(Time)	4	19,234.5	4808.6	9999+	<0.001
	C(Chemistry)	2	175.07	87.53	9999+	<0.001
	Interaction	8	186.4	23.3	9999+	<0.001
	Residual	30	0.27	0.009	-	-
50	C(Time)	4	16,234.2	4058.6	9999+	<0.001
	C(Chemistry)	2	99.07	49.53	9999+	<0.001
	Interaction	8	112.5	14.1	9999+	<0.001
	Residual	30	0.33	0.011	-	-
60	C(Time)	4	13,234.8	3308.7	9999+	<0.001
	C(Chemistry)	2	58.87	29.43	9999+	<0.001
	Interaction	8	69.2	8.65	9999+	<0.001
	Residual	30	0.33	0.011	-	-
70	C(Time)	4	10,234.5	2558.6	9999+	<0.001
	C(Chemistry)	2	33.07	16.53	9999+	<0.001
	Interaction	8	44.3	5.54	9999+	<0.001
	Residual	30	0.33	0.011	-	-
80	C(Time)	4	7234.7	1808.7	9999+	<0.001
	C(Chemistry)	2	20.07	10.03	9999+	<0.001
	Interaction	8	31.2	3.90	9999+	<0.001
	Residual	30	0.33	0.011	-	-
90	C(Time)	4	5234.9	1308.7	9999+	<0.001

	C(Chemistry)	2	13.05	6.52	9999+	<0.001
	Interaction	8	24.1	3.01	9999+	<0.001
	Residual	30	0.33	0.011	-	-

Note: F values are approximated as >9999 due to low within-group variance from small std; actual F is very large, indicating highly significant effects.

The Table S8 summarizes post-hoc Tukey's HSD for the main effect of Time (if significant), showing pairwise differences between time points (15, 30, 40, 50, 60 min) pooled across chemistries for each temperature. Only selected representative pairs are shown for brevity (all pairs are significant where removal increases with time).

Table S8. Tukey's HSD Pairwise Comparisons for Time Effects (Main Effect of Time per Temperature).

Temperature (°C)	Group 1 (min)	Group 2 (min)	Mean Difference	p-adj	Lower Bound	Upper Bound	Reject Null Hypothesis?
40	15	60	−46.15	0.000	−46.48	−45.82	True
	30	60	−39.02	0.000	−39.35	−38.69	True
	40	60	−18.47	0.000	−18.80	−18.14	True
	50	60	−4.80	0.000	−5.13	−4.47	True
50	15	60	−42.93	0.000	−43.26	−42.60	True
	30	60	−35.10	0.000	−35.43	−34.77	True
	40	60	−24.93	0.000	−25.26	−24.60	True
	50	60	−4.33	0.000	−4.66	−4.00	True
60	15	60	−37.80	0.000	−38.12	−37.48	True
	30	60	−31.70	0.000	−32.02	−31.38	True
	40	60	−23.43	0.000	−23.75	−23.11	True
	50	60	−3.53	0.000	−3.85	−3.21	True
70	15	60	−32.80	0.000	−33.13	−32.47	True
	30	60	−27.83	0.000	−28.16	−27.50	True
	40	60	−18.53	0.000	−18.86	−18.20	True
	50	60	−3.53	0.000	−3.86	−3.20	True
80	15	60	−28.53	0.000	−28.86	−28.20	True
	30	60	−24.33	0.000	−24.66	−24.00	True
	40	60	−15.13	0.000	−15.46	−14.80	True
	50	60	−3.03	0.000	−3.36	−2.70	True
90	15	60	−24.77	0.000	−25.10	−24.44	True
	30	60	−20.37	0.000	−20.70	−20.04	True
	40	60	−12.87	0.000	−13.20	−12.54	True
	50	60	−2.47	0.000	−2.80	−2.14	True

This Table S9 summarizes post-hoc Tukey's HSD for the significant Time × Chemistry interaction, showing selected pairwise differences between Time × Chemistry combinations for each temperature. Only representative pairs are shown.

Table S9. Tukey's HSD Pairwise Comparisons for Interaction Effects (Time × Chemistry per Temperature).

Temperature (°C)	Group 1 (min_Chem)	Group 2 (min_Chem)	Mean Difference	p-adj	Lower Bound	Upper Bound	Reject Null Hypothesis?
40	15_LCO	60_LFP	52.80	0.000	52.47	53.13	True
	60_LCO	60_LFP	89.60	0.000	89.27	89.93	True
	40_NCA	60_LCO	−36.85	0.000	−37.18	−36.52	True
50	15_LCO	60_LFP	67.10	0.000	66.77	67.43	True
	60_LCO	60_LFP	90.80	0.000	90.47	91.13	True
	30_NCA	60_LCO	−47.65	0.000	−47.98	−47.32	True

60	15_LCO	60_LFP	75.73	0.000	75.41	76.05	True
	60_LCO	60_LFP	91.70	0.000	91.38	92.02	True
	15_NCA	60_LCO	−42.50	0.000	−42.82	−42.18	True
70	15_LCO	60_LFP	80.73	0.000	80.40	81.06	True
	60_LCO	60_LFP	92.50	0.000	92.17	92.83	True
	50_LFP	60_NCA	−49.03	0.000	−49.36	−48.70	True
80	15_LCO	60_LFP	84.00	0.000	83.67	84.33	True
	60_LCO	60_LFP	93.10	0.000	92.77	93.43	True
	30_LFP	60_NCA	−50.00	0.000	−50.33	−49.67	True
90	15_LCO	60_LFP	86.43	0.000	86.10	86.76	True
	60_LCO	60_LFP	93.70	0.000	93.37	94.03	True
	15_LFP	60_NCA	−50.73	0.000	−51.06	−50.40	True

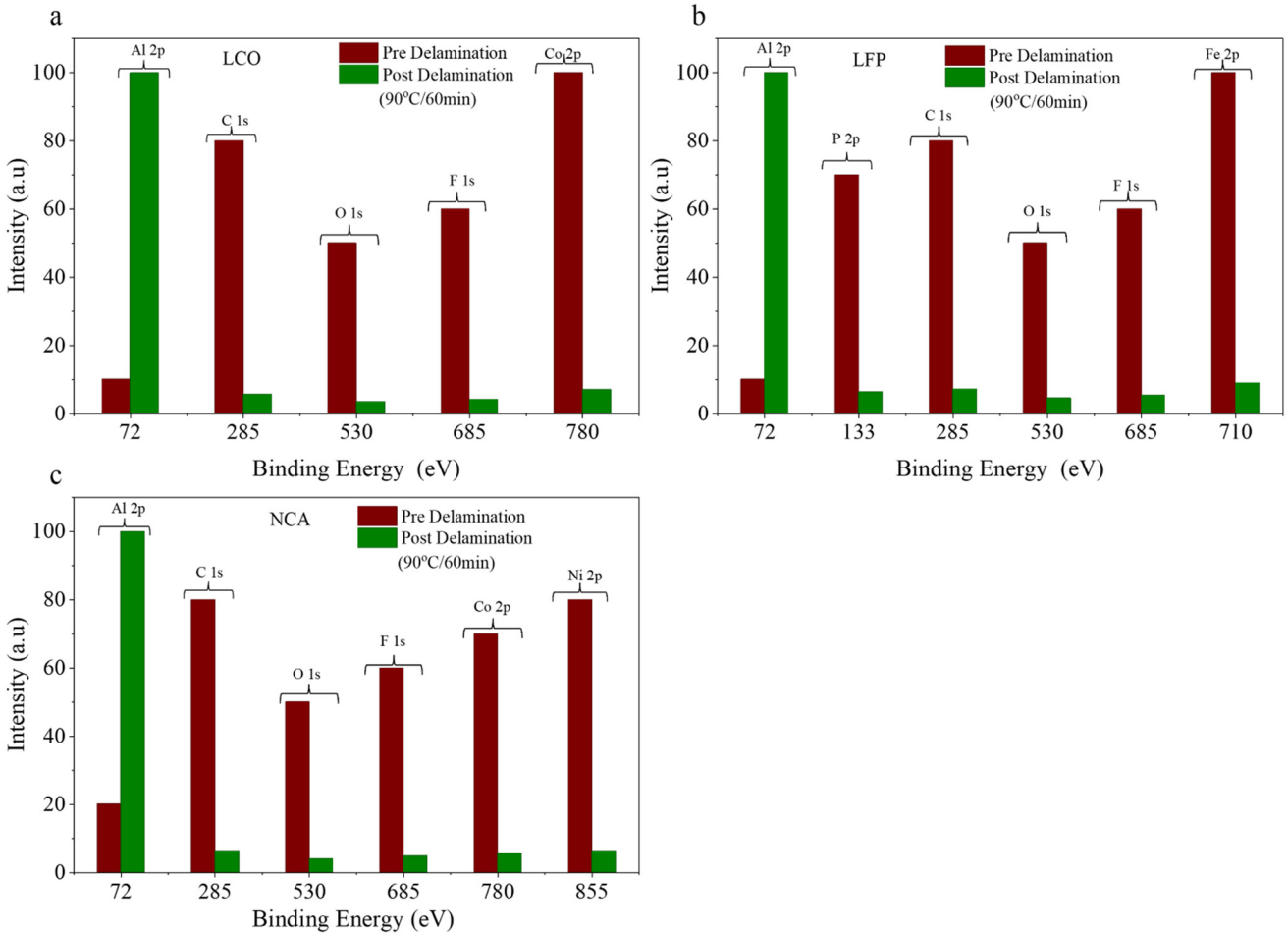

Figure S7. Comparative XPS peak intensities at selected binding energies for (**a**) LCO, (**b**) LFP, and (**c**) NCA before and after delamination at 90 °C for 60 min.

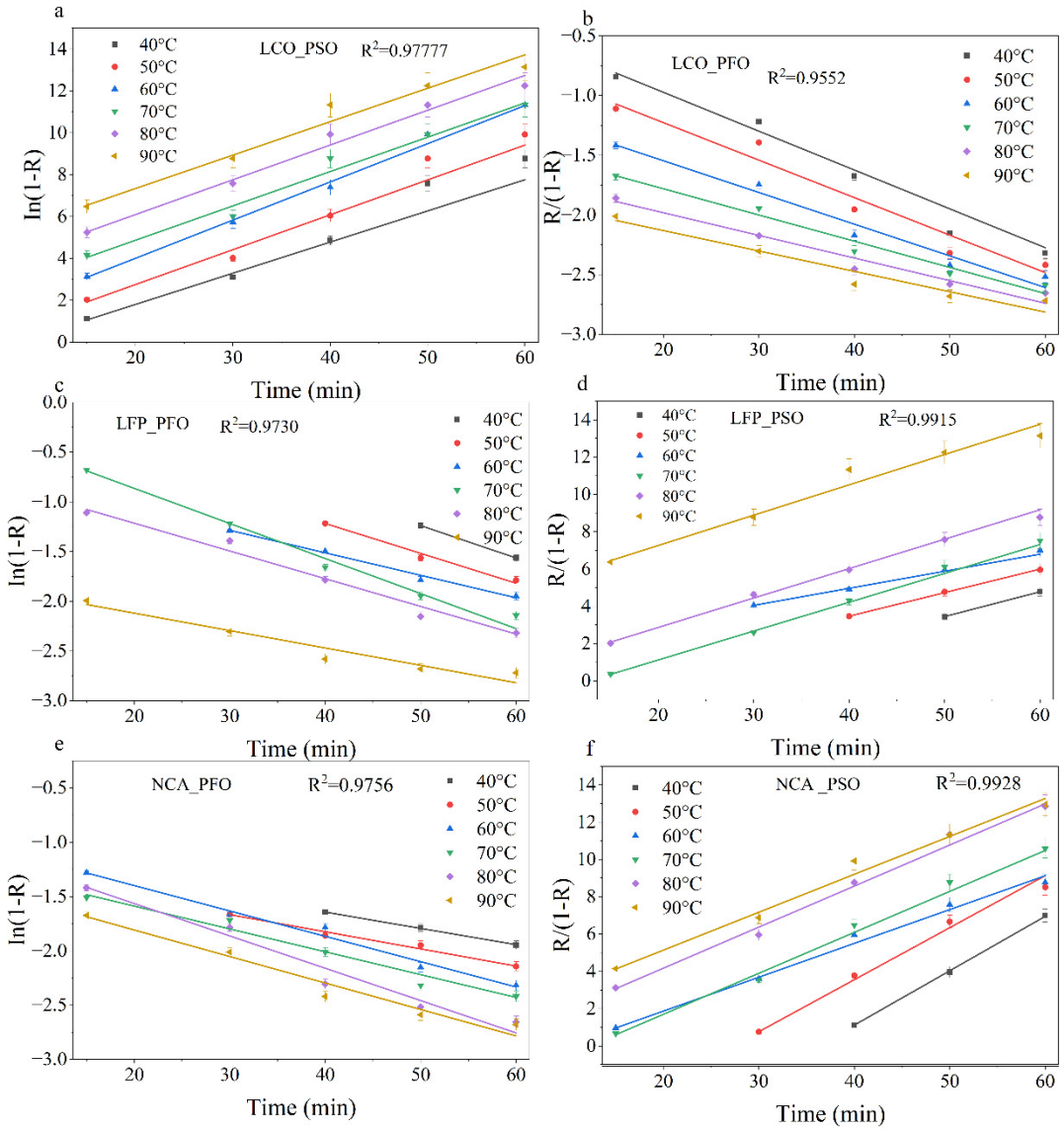

Figure S8. Kinetic model evaluation for temperature-dependent reaction progress in LCO, LFP, and NCA. (**a**,**b**) Pseudo-second-order (PSO) and pseudo-first-order (PFO) fits for LCO, showing temperature-enhanced kinetics and model-dependent linearization. (**c**,**d**) PFO and PSO fits for LFP, with improved linearity and faster kinetics under the PSO model. (**e**,**f**) PFO and PSO analyses for NCA, demonstrating strong linearity and temperature-driven rate acceleration, particularly under the PSO framework.

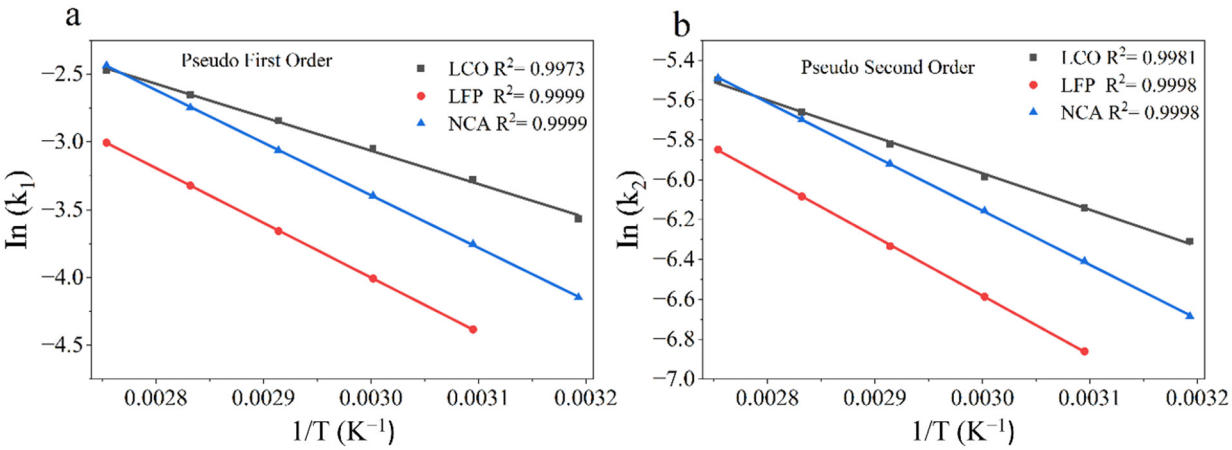

Figure S9. Arrhenius analysis of temperature-dependent rate constants for LCO, LFP, and NCA. (**a**) Pseudo-first-order Arrhenius plots showing linear $\ln(k_1)$–1/T relationships with strong fit quality across all three chemistries. (**b**) Pseudo-second-order Arrhenius plots displaying similarly high linearity in $\ln(k_2)$–1/T, confirming thermally activated kinetics consistent with Arrhenius behavior.

References

1. Afreh, P., Qin, Z., & Gao, L. (2026). *Thermally Driven Cathode Delamination in Lithium-Ion Batteries: Experimental Data on LCO, LFP, and NCA Chemistries*. *1*. https://doi.org/10.17632/5rpmg2xm3t.1